SEISMIC DESIGN OF A BASE ISOLATED BUILDING IN THE VICINITY OF A HYPOTHETICAL M8 EARTHQUAKE IN SUBDUCTION ZONE

Yoe MASUZAWA [1]
Saburoh MIDORIKAWA [2], Hiroaki YAMANAKA [3], Yoshiaki HISADA [4]
Shouichi YAMAGUCHI [5], Mitsukazu KIMURA [6], Toshiyuki NAKAZAWA [7]
Tsuguhisa NISHIMURA [8] and Tsunehisa KOUNO [9]

SUMMARY

We introduced seismic design of a base isolated building in the proximity of a hypothetical M8 earthquake. Our seismic design is based on the assumption that an M8 Tokai earthquake will occur in the vicinity of the site in near future. In order to evaluate the regional ground properties, we performed the microtremor array survey (Yamanaka, 1995) and ground motion observation at and around the construction site. Based on the survey and observations, and comparing the advantages and disadvantages of the strong motion prediction methods available, the following evaluations were performed; 1. Empirical method (Kobayashi and Midorikawa, 1982). 2. Semi-empirical method (Irikura, 1986). 3. Theoretical method (Hisada, 2000).

The maximum amplitudes of the seismic wave calculated using the three methods are as follows; Empirical method: 498cm/sec^2, 36cm/sec, 13cm. Semi-empirical method: 350cm/sec^2, 25cm/sec, 16cm. Teoretical method: 542cm/sec^2, 80cm/sec, 56cm.

Because of directivity effect, near source long period pulses are generated using the theoretical method. As a result, theoretical results are larger than another two.

Satisfaction of the acceptability criteria was confirmed by conducting dynamic response analyses using the ground motion for aseismic design. The result of the response analysis, which was conducted under the worst scenario of theoretical method, revealed that the maximum shear coefficient of upper structure and the maximum deformation of seismic isolation interface are 0.202 and 44.6cm, respectively. It has been judged that the results could satisfy our acceptability criteria (0.205 and 50cm).

[1] *Department of Architecture, Yokogawa Architects & Engineers, Inc., 2-20-28, Shimomeguro, Meguro-ku, Tokyo 153-0064, JAPAN. E-mail: masuzawa@yae.co.jp*
[2] *Department of Built Environment, Tokyo Institute of Technology, 4259, Nagatsuda, Midori-ku, Yokohama 226-8502, JAPAN*
[3] *Department of Environmental Physics and Engineering, Tokyo Institute of Technology, 4259, Nagatsuda, Midori-ku, Yokohama 226-8502, JAPAN*
[4] *Department of Architecture, Kogakuin University, 1-24-2, Nishi-Shinjyuku, Shinjyuku-ku, Tokyo 163-8677, JAPAN. E-mail: hisada@cc.kogakuin.ac.jp*
[5] *Tokyo-kenchiku Structural Engineers, 20, Shinano-machi, Shinjyuku-ku, Tokyo 160-0061, JAPAN*
[6] *Tokyo-kenchiku Structural Engineers, 20, Shinano-machi, Shinjyuku-ku, Tokyo 160-0061, JAPAN*
[7] *Tokyo-kenchiku Structural Engineers, 20, Shinano-machi, Shinjyuku-ku, Tokyo 160-0061, JAPAN*
[8] *Department of Architecture, Yokogawa Architects & Engineers, Inc., 2-20-28, Shimomeguro, Meguro-ku, Tokyo 153-0064, JAPAN.*
[9] *Department of Architecture, Yokogawa Architects & Engineers, Inc., 2-20-28, Shimomeguro, Meguro-ku, Tokyo 153-0064, JAPAN.*

INTRODUCTION

The building reported herewith is a large-scale medical complex for the surrounding communities. In order to ensure its functions and operations even the case of emergency, the building is required to feature a sufficient level of seismically-resistant performance. With the structural design objective in mind, we set acceptability criteria which should be satisfied with.

The site is located in Sizuoka prefecture, Tokai area, Japan, a region where an M7-M8 subduction zone or active faulting earthquake is likely to occur. We were determined that it would be impossible to achieve the objectives by using an ordinary seismically-resistant structure.

To cope with the problem, we came up with a base isolation structure with a longer natural period in order to reduce the seismic acceleration input effectively. Even after the severest possible earthquake motion, the building must guarantee the internal medical and first-aid activities.

In a base-isolated building design, it is important to acknowledge not only the maximum amplitudes of the ground motions but also the spectral amplitudes at the natural period of the base-isolated building vibration.

The seismic ground motion was determined in accordance with the characteristics of the assumed earthquake and the ground properties of the site. The data of the ground motion, then, was taken into the design concept.

SUMMARY OF BUILDING

The building concerned is a large-scale medical complex with eleven stories, one basement and a penthouse. The building, with an eaves height of 53.45 meters, has 630 beds for hospitalized patients and other necessary medical care units. The structure is a steel/reinforced concrete (partially constructed with steel). The engineering highlight lies in a seismic isolation interface between the upper and under structures (with a partial basement (a base-isolation method in the intermediate layer)). The plan and framing elevation of the building are shown in **Figure 1**.

The structural design for the upper and base structures fully complied with; the Building Standard Law, the Building Standard Law Enforcement Order, various criteria specified by the Building Center of Japan and Architectural Institute of Japan, as well as the Architectural Structure Design Index and Descriptions issued by Shizuoka prefectural government.

PERFORMANCE OBJECTIVE AND ACCEPTABILITY CRITERIA

As earthquake motion input levels, the following two levels were established and used;

Level 1: A earthquake motion level that would probably affect the building in the site more than one time during its lifetime.

Level 2: The severest earthquake motion level that would possibly affect the building during its lifetime.

The performance objectives were set as follows, in relation to the levels above;

	Level 1	Level 2
Structural Element:	Fully operational	Operational (usable with light repair)
Non-structural Element:	Fully operational	Operational (usable with light repair)
Facilities / Equipment:	Fully operational	Operational (major facilities and equipment to be still operable after earthquake occurrence)

The acceptability criteria set during the design phase are shown in **Table 1**.

The horizontal floor response acting on the hospital ward floors (4 - 10 floors) were set at approximately 300 cm/sec^2 because the fundamental functionality would not be maintained even though the structure remains operational.

GROUND PROPERTIES

The site inclines from north toward south. The geologic stratum consists of the loamy layer as the ground surface and the tuff layer containing gravel and rocks under the loam. The latter is further separable into three layers, and the whole building is supported by the top layer of the tuff. The depth of the tuff layer is more than 60m from the ground surface. It allows the S-wave velocity exceeding 600m/sec. No underground water has been found nearby.

In order to evaluate the deep ground properties, the microtremor array survey (Yamanaka, 1995) were performed at and around the construction site. As a result of the survey and analysis, geologic structure of S-wave velocity and S-wave amplification over the bed rock on earthquake wave traveling are explained. These shown in **Figure 3** and **Figure 4**.

GROUND MOTION FOR ASEISMIC DESIGN

Our seismic isolation design was based on the assumption that an M8-class subduction-zone earthquake would occur in the vicinity of the site. The assumption derived from the following considerations; 1) the history of earthquakes in the region and 2) the existence of active faults in the region. Construction site and surrounding faults are shown in **Figure 2**. Considered influence of these earthquakes, Tokai earthquake was adopted a target earthquake.

There have been, however, few records of the near-source strong ground motion of the M8 earthquake.

Based on the microtremor array survey, and considering the advantages and disadvantages of the strong motion prediction methods available, the following all evaluations were conducted;

1. Empirical method (Kobayashi and Midorikawa, 1982).
2. Semi-empirical method (Irikura, 1986).
3. Theoretical method (Hisada, 2000).

The list of simulated waves are provided in **Table 2**. It is mentioning here that the values and status of the simulated seismic motions largely fluctuated due to the difference in methods used, even though they were generated based on the identical earth fault. This is caused by directivity effect, near source long period pulses are generated using the theoretical method.

In addition to the seismic wave uniquely produced considering the regional nature properties, several observed records which have been widely utilized were adopted for our analysis.

As reference values for the input level, a statistical approach using the earthquake database was undertaken to obtain socially-accepted values as well as our prediction.

The very rare level, in order for confirming the margin of safety of the building, was also established.

The list of observed records are provided in **Table 3**. Time history of acceleration and velocity are shown in **Figure 5**. Also psudo-velocity response spectra of the simulation seismic motions are represented by **Figure 6**.

DESCRIPTION OF SEISMIC ISOLATION DEVICES

The seismic isolation devices used for the building were; rubber bearings with a diameter of 800mm, four types of read plugged rubber bearings and featuring diameters of 800mm, 900mm, 1000mm and 1100mm, respectively, two different sliding supports with diameters of 300mm and 400mm, and steel dampers with a loop diameter of 760mm.

The rubber bearing provides great rigidity and resistance capability against vertical load applications; whereas it reacts more flexibly against horizontal load inputs which results in a great deflection in the longitudinal direction.

The sliding support, as the name implies, begins sliding under a certain horizontal load application whereby static friction of the element yields to the load. Under the condition, it maintains the horizontal force at a predetermined level due to its slidability.

Both the steel damper and lead plug are damping elements utilizing the plasticity deflection of the steel and lead materials. The latter promotes an earlier yield when compared with the former. Because of the characteristics, it ensures a sufficient damping performance even under a relatively small deflection. The steel damper provides a stable damping performance under a large deflection condition.

By combining the two different damping characteristics, motions of the building due to microtremors and/or winds are coped with by rigidities of the two elements. In the case of a small earthquake occurrence, plastic deflection of the lead plug absorbs the seismic energy. Under a severe earthquake, a combined plastic deflections of the steel damper and lead plug absorb the energy.

Immediately under the columns, 241 base-isolation supporting elements were integrated, consisting of 209 rubber bearings and 32 sliding supports. There are 60 steel dampers used.

The location of the dampers were aligned that the center of gravity of the upper structure and the center of rigidity of the seismic isolation interface come closest possible to each other. Furthermore, to ensure torsional rigidity necessary for the building, the dampers were placed at the peripheral area of the building.

DESCRIPTION OF DYNAMIC RESPONSE ANALYSIS

Satisfaction of the acceptability criteria was to be confirmed by conducting dynamic analyses using the ground motion for aseismic design and levels assumed above.

For the analysis, a lumped mass model consisting of 13 lumped mass were designed. Each of 13 lumped mass represents each floor. Since the basement features a sufficient level of rigidity, it was integrated with the ground

floor when modeled under the assumption that the basement would move identically to the floor above. Prior to the dynamic analysis, we had confirmed that the effect of torsional stress was negligibly small by conducting the natural frequency observation. Stiffness dispersion of seismic isolation devices was 30% considered, because seismic isolation structure is sensitive to the period of earthquake vibration.
The performance requirements for the upper structure is shown in **Table 4**, those for the seismic isolation elements in **Table 5**.
Also, the analytical results of the seismic response are shown in **Figure 7**.
The maximum responsive bearing force was measured at 23 N/mm^2 or less even with a static consideration of the vertical motion (0.5G). The result fit our target with a sufficient margin. No damage will be caused to the rubber bearing under the minimum responsive bearing force condition where tensile force rated at around $-1.1N/mm^2$ was generated without the vertical motion considered.
The results of acceptability criteria, the input level threshold where fatal damage begins to occur to the medical functions and operations, and margin of safety of the building are provided in **Table 6**. Upper structure came to within elastic strength and seismic isolation interface controlled within performance-ensureable deformation toward near source long period pulses.

CONCLUSIONS

We succeeded seismic design of a base isolated building in the proximity of a hypothetical M8 earthquake.
Satisfaction of the acceptability criteria was confirmed by conducting dynamic response analyses using the ground motion for aseismic design. The result of the response analysis, which was conducted under the worst scenario of theoretical method, revealed that the maximum shear coefficient of upper structure and the maximum deformation of seismic isolation interface are 0.202 and 44.6cm, respectively. It has been judged that the results could satisfy our acceptability criteria (0.205 and 50cm).
Thanks to the systematic and strategic use of braces and other materials, the horizontal floor response at the ward floors was recorded at approximately 345 gal. Though the value exceeded our target by approximately 15%, we are convinced that the seismically resistant design of the structure is successful.
The deflections of the seismic isolation devices were within the limit of safety under Level 1 condition (previously observed records). Under the severer level as well as the additional confirmation of safety margin, the deflections did not exceed the deflection threshold where the functions and operations of the hospital cannot be guaranteed.

ACKNOWLEDGEMENTS

This project was totally supported by Sizuoka prefecture. The cooperation of Nagaizumi high school is greatly improved this research.

REFERENCES

Hisada, Y. (2000), "A Hybrid Method for Predicting Strong Ground Motions at Broad-frequencies Near M8 Earthquakes in Subduction Zones", *12wcee2000, 763/4/A*.
Irikura, K. (1986), "Prediction of Strong Acceleration Motion using Empirical Green's Function", Proc. 7th Japan Earthq. Engng. Sym., pp.151-156
Kobayashi, H., Midorikawa, S. (1982), "A Semi-empirical Method for Estimating Response Spectra of Near-field Ground Motions with Regard to Fault Rupture", Proc. 7th European Conference of Earthq. Engng., pp.161-168.
Yamanaka, H., Ishida, H. (1995), "Phase Velocity Inversion Using Genetic Algorithms", J. Struct. Constr. Eng., AIJ, No. 468, pp.9-17.

Table 1: Acceptability criteria of building

		Level 1	Level 2		Very rare level
			Observed record	Simulated wave	
Acceptability criteria	Upper structure	A	A	B	B
	Seismic isolation device	A	A	B	B
	Under structure	A	A	B	B

Upper/Under structure: A(within working stress), B(within elastic strength), C(within ultimate strength)
Seismic isolation device: A(within safety deformation), B(within performance-ensureable deformation), C(within ultimate deformation)

Table 2: List of simulated waves

Method	Amax (cm/sec^2)	Vmax (cm/sec)	Dmax (cm)
Empirical (M-KEIKEN)	497.6	36	13
Semi-empirical (M-GOUSEI)	349.9	25	16
Theoretical (M-MEXIC1)	392.5	64	52
Theoretical (M-CHILI1)	480.5	80	56

Table 3: List of observed records

	Original wave		Standardized maximum acceleration (cm/s^2)		
	Vmax (cm/s)	Amax (cm/s^2)	Level1(25cm/s)	Level2(50cm/s)	Very rare(75cm/s)
EL CENTRO 1940 NS	33.5	341.7	255	511	766
TAFT 1952 EW	17.7	176.0	248	497	745
HACHINOHE 1968 NS	34.1	225.0	165	330	780

Table 4: Performance requirements of upper structure

		Max. working stress	Max. elastic strength
X direction	Base shear coefficient	0.15	0.205
	Max. story deflection angle	1/505	1/310
Y direction	Base shear coefficient	0.15	0.225
	Max. story deflection angle	1/439	1/204

Table 5: Performance requirements of seismic isolation devices

			Safety deformation	Performance-ensureable	Ultimate deformation
Rubber bearing	800A	deformation(cm)	36.0	54.0	72.0 (64.0)
		Shear strain	200%	300%	400%
	800B	deformation(cm)	40.3	60.5	80.6 (64.0)
		Shear strain	200%	300%	400%
Lead plugged rubber bearing	1200	deformation(cm)	39.6	60.0	96.0 (72.0)
		Shear strain	165%	250%	400%
	1100	deformation(cm)	37.0	56.0	89.6 (80.0)
		Shear strain	165%	250%	400%
	900	deformation(cm)	33.2	50.4	80.6 (72.0)
		Shear strain	165%	250%	400%
	800	deformation(cm)	33.2	50.4	80.6 (64.0)
		Shear strain	165%	250%	400%
Sliding support		deformation(cm)	40.0	50.0	60.0
Steel dumper		deformation(cm)	45.0	60.0	70.0

* Numbers in parentheses represent deformations under buckling.

Table 6: Margin of safety with upper structure and seismic isolation devices

		Level 2 (Observed records)	Level 2 (Simulated waves)	Very rare level
Acceptability criteria	Upper structure Base shear coeficient	A CB=0.150	B CB=0.205	B CB=0.205
	Seismic isolation device Deformation(Shear strain)	A 33cm(165%)	B 50cm(250%)	B 50cm(250%)
Results of dynamic response analysis	Upper structure	0.119	0.202	0.178
	Seismic isolation device	20.1cm	44.6cm	39.9cm
Margin of safety (Result/Criteria)	Upper structure	0.119/0.150=0.79	0.202/0.205=0.98	0.178/0.205=0.87
	Seismic isolation device	20.1/33.2=0.61	44.6/50.4=0.88	39.9/50.4=0.79

Upper: A(within working stress), B(within elastic strength), C(within ultimate strength)
Seismic isolation device: A(within safety deformation), B(within performance-ensureable deformation), C(within ultimate deformation)

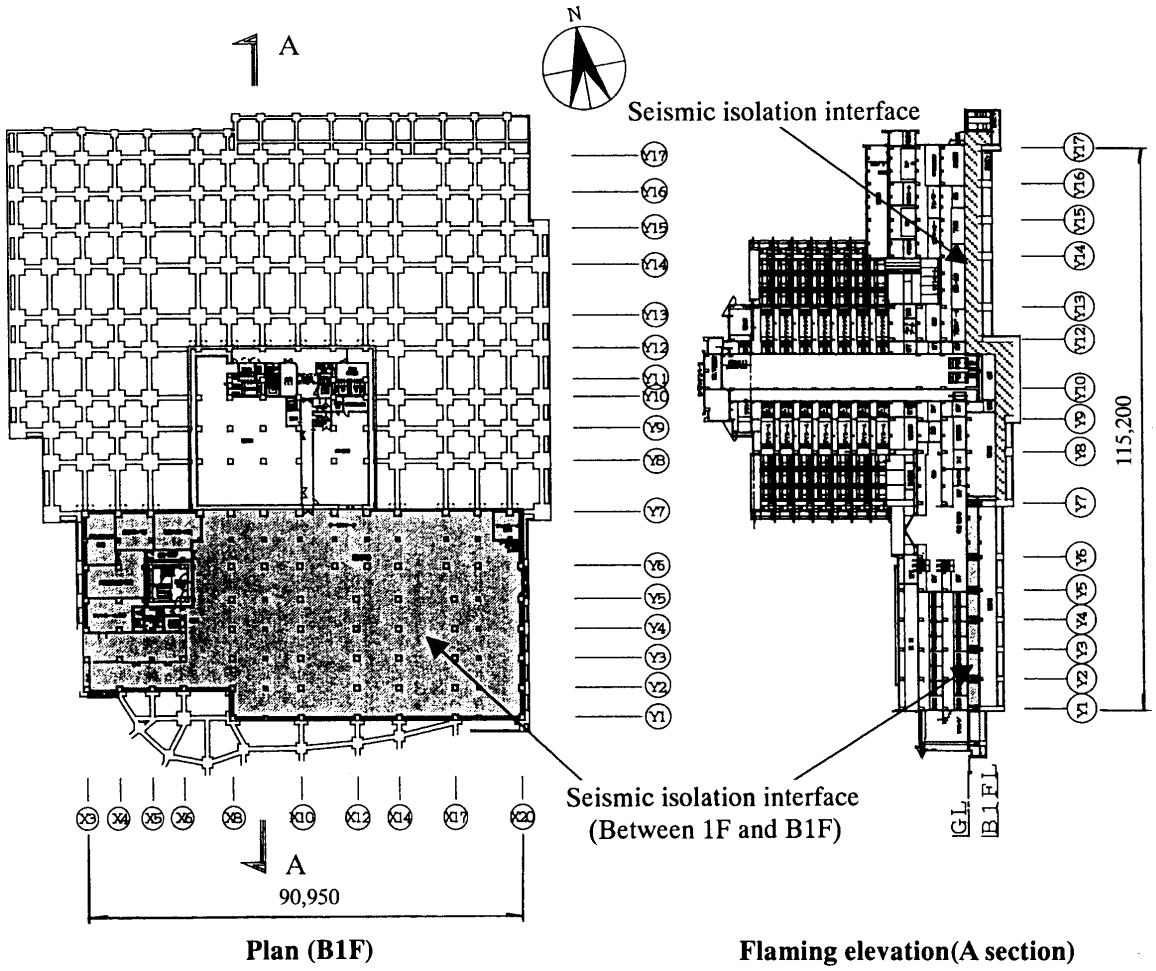

Figure 1. Plan and framing elevation

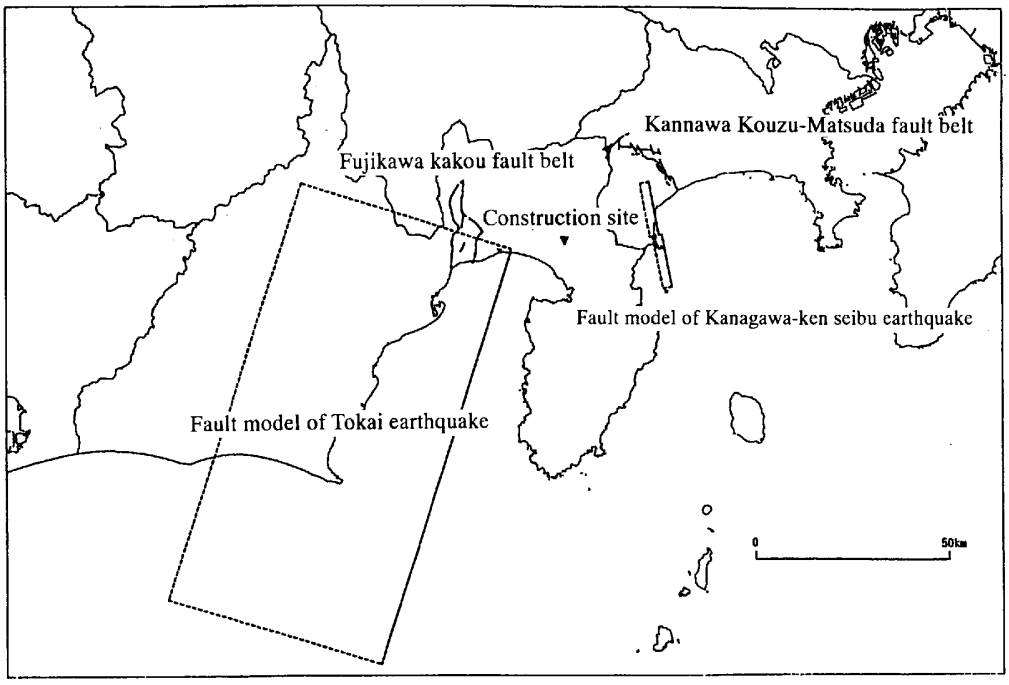

Figure 2. Construction site and surrounding faults

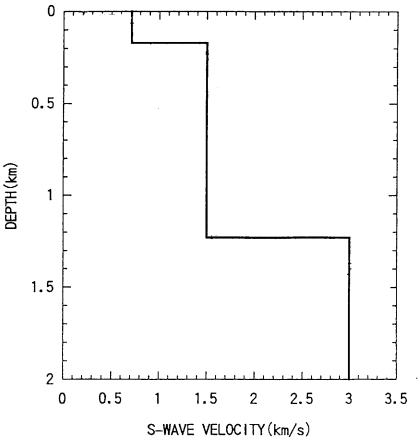

Figure 3. S-wave velocity structure

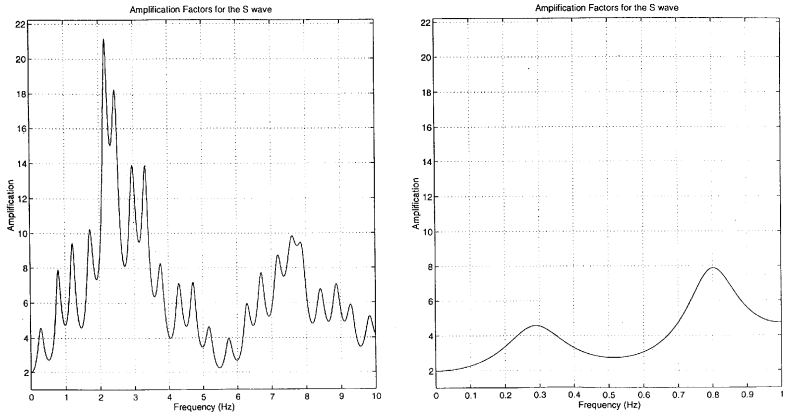

Figure 4. S-wave amplification over the bed rock on earthquake wave travelling

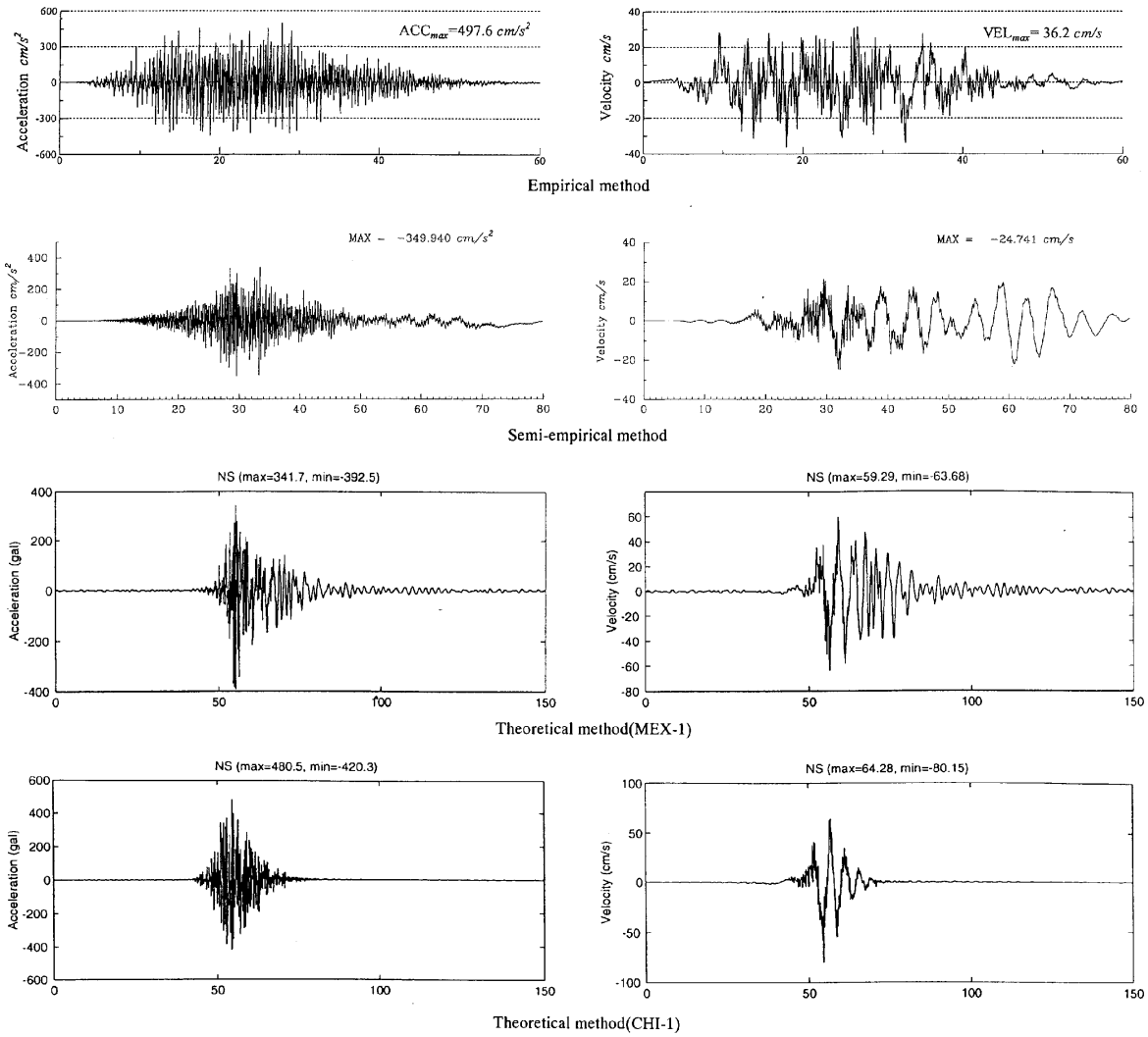

Figure 5. Simulated acceleration and velocity at the construction site

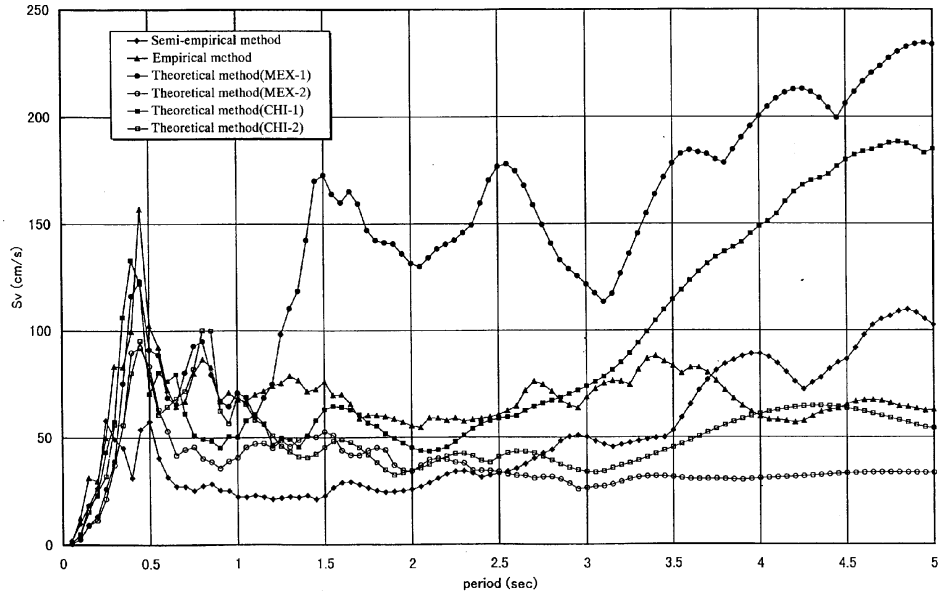

Figure 6. Velocity response spectra of simulated waves

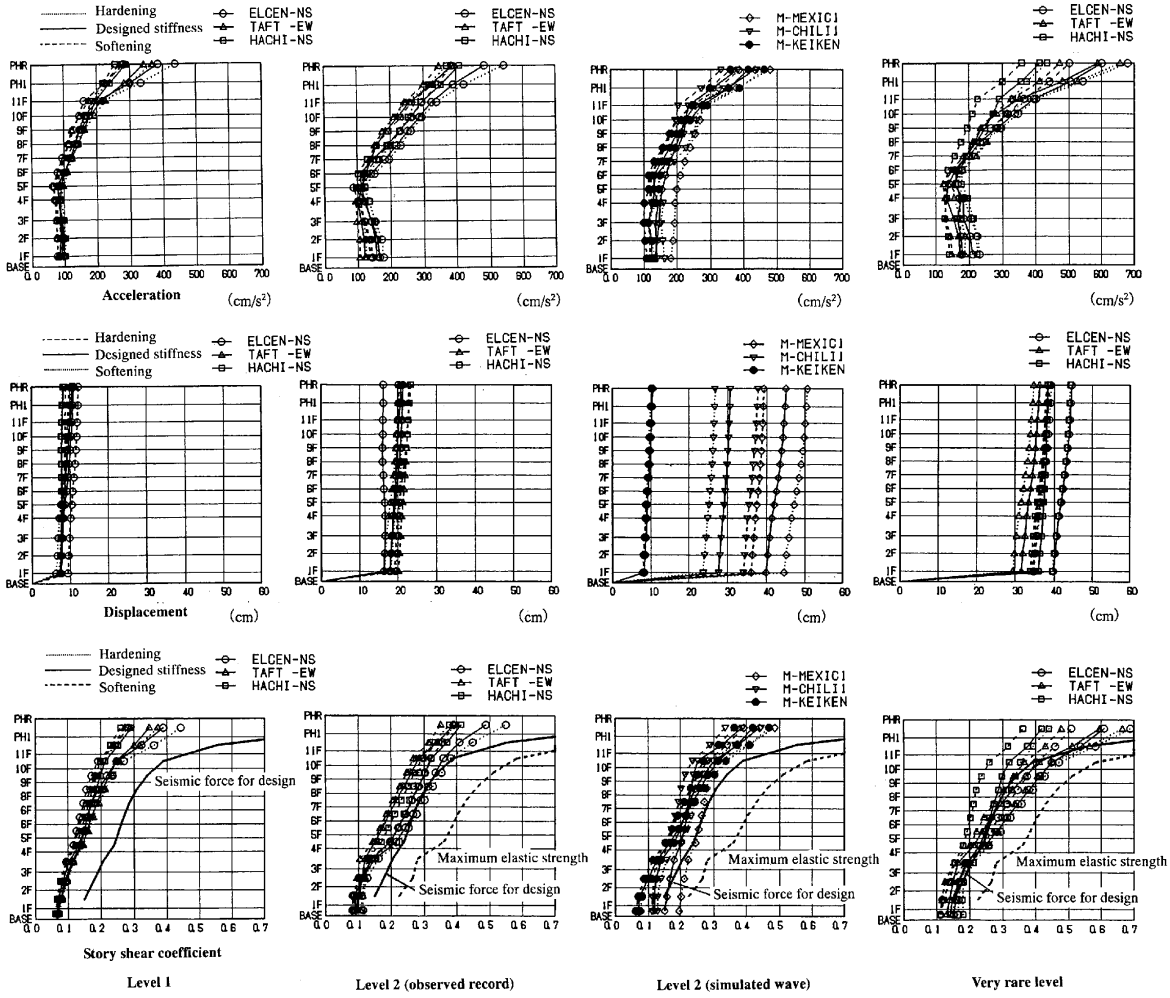

(X direction)

Figure 7. Results of dynamic response analysis